Zeitschrift: Schweizerische mineralogische und petrographische Mitteilungen = Bulletin suisse de minéralogie et pétrographie

Band: 68 (1988)

Heft: 2

Artikel: Metasomatic zonation of REE in zirconolite from a marble skarn at the Bergell contact aureole (Switzerland / Italy)

Autor: Williams, C. Terry / Gieré, Reto

DOI: https://doi.org/10.5169/seals-52055

SCHWEIZ. MINERAL. PETROGR. MITT. 68, 133-140, 1988

Metasomatic zonation of REE in zirconolite from a marble skarn at the Bergell contact aureole (Switzerland / Italy)

by *C. Terry Williams*[1] and *Reto Gieré*[2]

Abstract

Zirconolite from a marble skarn at the Bergell contact aureole (Switzerland / Italy) has been re-examined, and the mineral chemistry more completely characterised. Three discrete zones were observed in the zirconolite, each possessing a distinctive chemical composition, and representing a zonal sequence of crystallisation. The concentrations of REE are markedly different in each zone, and reflect a progressive enrichment of heavy REE in the metasomatic fluid during the alteration of the skarn. Tungsten is reported for the first time in zirconolites, and is present at minor concentration levels in all three zones.

Keywords: Zirconolite, Rare Earth Elements, Metasomatic Zonation, Skarn, Bregaglia contact aureole, Switzerland, Italy.

Introduction

Zirconolite in a marble skarn from the Bergell contact aureole (Switzerland / Italy) has been described originally by GIERÉ (1986). The low analytical totals obtained for zirconolite in his original study (96.1% from 15 elements) indicated that undetermined elements may be present at minor concentration levels. In order to make a full chemical characterisation of zirconolite, a sample of the marble skarn was resectioned and, from a selection of ten polished thin sections, eleven zirconolite grains were analysed by electron probe microanalysis to cover a range of 31 elements. This note details the results, and provides new information on the mineral chemistry of zirconolite, and on the chemistry of the metasomatic fluid present, particularly for the rare earth elements (REE), during the alteration of the skarn.

Mineralogy and Geological Setting

The detailed mineralogy and geological setting of the skarn were given by GIERÉ (1986), but they are briefly summarised here. The marble skarn occurs at the eastern margin of the Tertiary Bergell calc-alkaline igneous intrusion where gneisses and marbles are cross-cut at their contact by the Bergell granodiorite (BUCHER-NURMINEN, 1977, 1981: GIERÉ, 1985). The skarn is an assemblage of mainly spinel, phlogopite and anorthite, with relic calcite and accessory rare earth-bearing minerals zirconolite, allanite and sphene. Textural relationships indicate a step-wise three-stage alteration of the spinel to 1) högbomite or corundum + magnetite, 2) margarite, and 3) chlorite (GIERÉ, 1986). Of the rare earth-bearing minerals, zirconolite is the most common, although modally not more than 0.1%. Optically zirconolite

[1] Department of Mineralogy, British Museum (Natural History), Cromwell Road, London SW7 5BD, U.K.

[2] Institut für Mineralogie und Petrographie, ETH-Zentrum, CH-8092 Zürich, Switzerland. Present address: Department of Geological Sciences, University of British Columbia, Stores Road 6339, Vancouver, B.C. Canada V6T 2B4.

Tab. 1 Inter-element correction factors used in the analysis of zirconolites

Element Interfered with	Crystal	Peak Position (θ)	Interfering radiation line	Peak Position(θ)	*Correction factor
Ba	PET(002)	18.52	Ti-$K\alpha_1$	18.33	0.02
Pr	LIF(200)	37.71	La-$L\beta_1$	37.64	0.303
Nd	LIF(200)	36.07	Ce-$L\beta_1$	35.81	0.011
Sm	LIF(200)	33.12	Ce-$L\beta_{2,1s}$	33.27	0.082
Gd	LIF(200)	30.55	Ce-$L\gamma_1$	30.59	0.090
"	"	30.55	La-$L\gamma_2$	30.54	0.026
Dy	LIF(200)	28.30	Mn-$K\beta_1$	28.32	0.338
W	LIF(200)	21.51	Yb-$L\beta_1$	21.50	0.51

* Correction Factor = concentration (weight %) of element interfered with equivalent to 1.0 weight % of interfering element.

varies from translucent reddish-brown to opaque, and is typically 30–40 μm in size.

Analytical Conditions

The zirconolites were analysed by a wavelength-dispersive electron microprobe (Cambridge Instruments Microscan 9) operated at 20 kV and with a specimen current of 25 nA measured on a Faraday cage. Thirty one elements were sought using well-characterised minerals, synthetic compounds or pure elements as standards. Data from all detected elements were fully corrected for ZAF matrix effects. Empirical corrections were calculated for spectral overlaps between interfering elements (Tab. 1). Considerable care was taken over the selection of background positions, particularly for the heavy REE, where intra-REE spectral interferences are potentially severe (ÅMLI and GRIFFIN, 1975).

Zirconolite

Zirconolite is polymorphous with the minerals zirkelite and polymignite, which are all essentially $CaZrTi_2O_7$ (MAZZI and MUNNO, 1983). Although structurally distinct, zirconolite can be distinguished from zirkelite only on the basis of weak intensity X-ray diffraction reflections obtained from single crystals (MAZZI and MUNNO, 1983) which, in natural samples, are often absent owing to partial or total metamictisation. The difficulties in distinguishing zirconolite from zirkelite in the absence of full X-ray characterisation have led to confusion in nomenclature (e.g. PLATT et al., 1987). Recently published guidelines by NICKEL and MANDARINO (1987, 1988), which recommend that the name zirconolite be replaced by zirkelite, do not however resolve the nomenclature problem. These guidelines were based on the nomenclature system for pyrochlore (HOGARTH, 1977), and were formulated before the confirmation of structural differences between zirconolite and zirkelite recognised by MAZZI and MUNNO (1983). In this study, the grains were too small to allow separation for single crystal X-ray diffraction, and the name zirconolite is retained such that its usage is consistent with that by GIERÉ (1986) in describing the original material.

Zirconolite has five cation-acceptor sites, these being Ca in 8-coordination, Zr in 7-coor-

Tab. 2 Electron microprobe analyses of zirconolites

	E1		E2		E3	
	average of 9	standard deviation	average of 3	standard deviation	average of 3	standard deviation
MgO	0.04	.04	<.04	-	0.07	.07
Al_2O_3	0.60	.06	0.74	.02	0.66	.03
SiO_2	0.09	.02	<.04	-	<.04	-
CaO	14.32	.87	11.34	.60	8.68	.77
TiO_2	39.3	1.70	33.5	.90	30.0	.50
MnO	0.01	.01	0.04	.03	0.09	.01
Fe_2O_3*	4.09	.66	6.34	.32	7.90	.36
Y_2O_3	0.58	.27	3.05	.09	7.23	.60
ZrO_2	34.5	.61	31.3	.68	29.2	1.27
Nb_2O_5	0.45	.09	1.82	.17	1.74	.22
La_2O_3	0.17	.02	0.11	.03	<.05	-
Ce_2O_3	0.99	.17	0.99	.28	0.23	.07
Pr_2O_3	0.09	.04	0.19	.03	<.09	-
Nd_2O_3	0.56	.12	1.39	.37	0.46	.27
Sm_2O_3	0.17	.10	0.58	.05	0.54	.04
Gd_2O_3	0.22	.03	0.67	.09	0.90	.08
Dy_2O_3	0.14	.10	0.61	.07	1.64	.21
Er_2O_3	0.14	.06	0.40	.05	1.20	.22
Yb_2O_3	<.1	-	0.33	.08	0.89	.12
HfO_2	0.55	.18	0.62	.19	0.62	.10
WO_3	0.70	.32	0.69	.19	0.95	.21
ThO_2	0.96	.81	2.51	1.74	1.12	.08
UO_2	0.37	.31	2.01	1.10	4.63	1.84
TOTAL	99.0		99.2		98.8	
$\Sigma^{(REE_2O_3)}_{(+\ Y_2O_3)}$	3.06		8.32		13.09	
	Number of cations based on 7 oxygens					
Ca	0.912		0.762		0.605	
Y	0.018		0.102		0.250	
La	0.004		0.003		0.000	
Ce	0.021		0.023		0.006	
Pr	0.002		0.004		0.000	
Nd	0.012		0.031		0.011	
Sm	0.004		0.012		0.012	
Gd	0.004		0.014		0.019	
Dy	0.003		0.012		0.034	
Er	0.003		0.008		0.025	
Yb	0.000		0.006		0.018	
Th	0.013		0.036		0.017	
U	0.005		0.028		0.067	
ΣCa site	1.001		1.041		1.064	
Zr	0.999		0.954		0.927	
Hf	0.009		0.011		0.011	
ΣZr site	1.008		0.965		0.938	
Mg	0.003		0.000		0.007	
Al	0.042		0.055		0.050	
Si	0.005		0.000		0.000	
Ti	1.756		1.579		1.468	
Mn	0.001		0.002		0.005	
Fe^{3+}	0.183		0.298		0.387	
Nb	0.012		0.051		0.051	
W	0.011		0.011		0.016	
ΣTi site	2.013		1.996		1.984	
TOTAL	4.022		4.004		3.986	

* All Fe as Fe_2O_3

F,Na,Cr,Sr,Mo,Ba,Ta,Pb all below 0.10 weight % as oxides

dination, and three distinct Ti sites: Ti(I) and Ti(III) are both 6-coordinate, and Ti(II) is 5-coordinate (GATEHOUSE et al., 1981; MAZZI and MUNNO, 1983). Data from both natural and synthetic zirconolite show that the structure allows a wide range of cation substitution (e.g. RINGWOOD, 1985), encompassing a variation in ionic size from 0.051 nm (Ti^{4+} in 5-coordination) to 0.112 nm (Ca^{2+} in 8-coordination) - all ionic radii data from SHANNON (1976) - and charge from 2+ (e.g. Mg, Mn) to 6+ (e.g. W). There is therefore potential for many elements to enter the zirconolite structure and, in the Bergell zirconolites described here, 23 elements are present at concentration levels above the detection limit of the electron microprobe (Tab. 2).

The secondary electron images obtained by the microprobe include a backscattered component which reveals atomic number contrast in some zirconolite grains, showing them to be distinctly zoned (fig. 1). Such zoning is not apparent in optical examination owing to the translucent to opaque nature of the zirconolite (GIERÉ, 1986). Microprobe spot and small raster areas (approximately 100 μm^2) were analysed for 31 elements on zoned and apparently homogeneous grains. Three separate zones were identified on the basis of their chemical compositions and are designated E1, E2 and E3. Each zone has a distinct chemical composition with relatively small standard deviations for the major elements (Tab. 2). With the exception of Th and U, for which there is considerable variation in concentration from grain to grain and in each zone, the concentrations with their standard deviations (SD) for the major elements in each zone, i.e. Ca, Ti, Zr and Σ (Y + REE), do not overlap those for the other zones, and the SD are greater than the 2 σ analytical errors for these elements (2 σ for Ca = 0.11; Ti = 0.24; Zr = 0.56, and Σ (Y + REE)

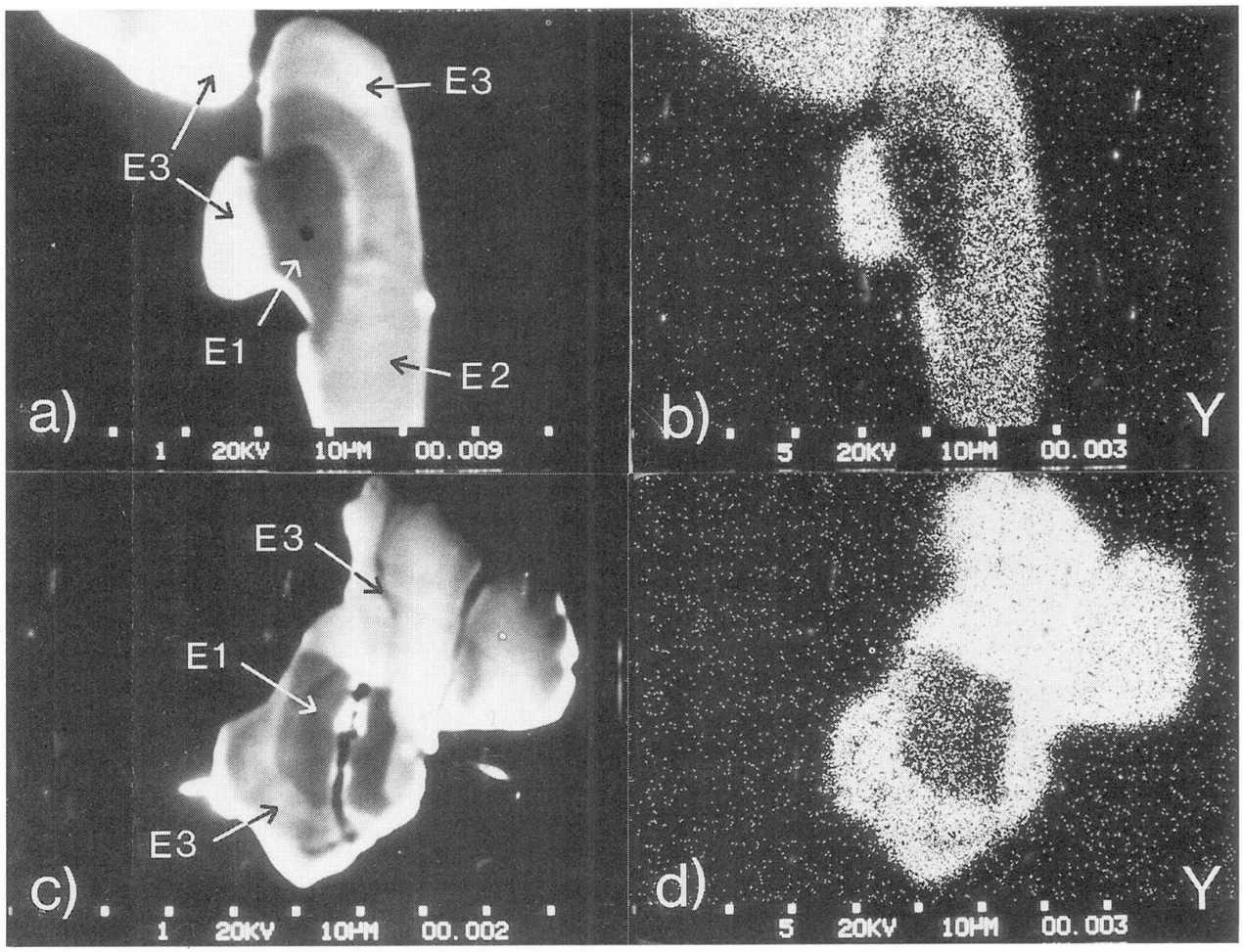

Fig. 1 a) Secondary electron image of zirconolite showing three zones E1, E2 and E3. b) X-ray distribution of Y. c) Secondary electron image of zirconolite displaying two zones E1 and E3. d) X-ray distribution of Y. Microprobe analytical conditions were 20kV and 25nA measured on a Faraday cage.

< 0.2). Of note are the relatively high concentrations of W (0.69–0.95% WO_3), a feature not previously reported for zirconolites from other localities.

Of the 11 grains analysed, only one displayed the three distinct zones (fig. 1a, b). Two other grains had two zones present, E1 + E2, and E1 + E3 (fig. 1c, d). All other grains analysed were of uniform composition: six of zone E1, and one each of zones E2 and E3. All analyses reported by GIERÉ (1986) represent zirconolite of E1 composition only. There is no correlation between the location of crystals with different zonal compositions and the composition of adjacent minerals.

The major chemical variations between zones E1, E2 and E3 are an increase in Σ (Y + REE) and Fe (as Fe_2O_3, GIERÉ, 1986), with a corresponding decrease in Ca, Ti and Zr (Tab. 2). No *continuous* zoning was observed in the major elements Ca, Ti, Fe, Zr, Y or REE between the three zones. The number of cations based on 7 oxygens was calculated (Tab. 2) following the procedure of GATEHOUSE et al. (1981) and KESSON et al. (1983), from which there can be seen to be a calculated excess of Ca, Y, REE, Th and U occupying the Ca site in zones E2 and E3, with a corresponding deficiency of Zr and Hf in the Zr site. Experimental work by KESSON et al. (1983) on synthetic zirconolite show that U^{4+} (0.095 nm), Y^{3+} (0.096 nm) and the middle to heavy REE Dy^{3+}, Er^{3+} and Yb^{3+} (0.097 nm, 0.094 nm and 0.0925 nm respectively, all in 7-coordination) can be accommodated in the Zr site (Zr^{4+} = 0.078 nm), with the light REE La^{3+}, Ce^{3+} and Nd^{3+} (0.116 nm, 0.114 nm and 0.1109 nm respectively in 8-coordination) strongly partitioned into the Ca site (Ca^{2+} = 0.112 nm). In order to attempt to redress the calculated cation imbalance in Ca and Zr sites of zones E2 and E3 (Tab. 2), it is suggested that U, with its similar charge to Zr is partitioned into the Zr site in preference to Y or heavy REE. Based on this assumption, the cations can be recalculated whereby Σ Ca = (Ca + Th + Y + REE) and Σ Zr = (Zr + Hf + U), and values close to 1.000 are obtained for each of E2 and E3, i.e. ΣCa_{E2} = 1.013, ΣCa_{E3} = 0.997 and ΣZr_{E2} = 0.993, ΣZr_{E3} = 1.005.

With Y and REE (and Th) occupying the Ca site, charge balance can be achieved by the substitution of divalent (e.g. Mg, Mn) or trivalent (e.g. Al, Fe^{3+}) cations for tetravalent Ti

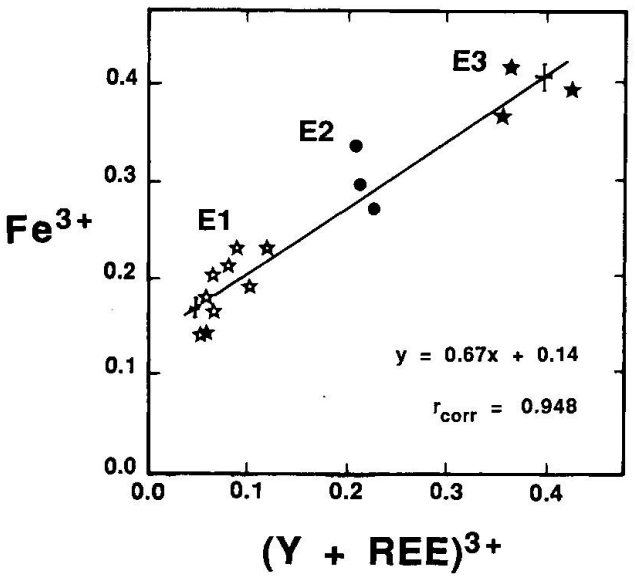

Fig. 2 Plot of Fe^{3+} against $(Y + REE)^{3+}$ cations for the three zones E1, E2 and E3. Error bars represent 2σ errors resulting from counting statistics.

(RINGWOOD, 1985). Since Mg, Mn and Al remain relatively constant at low concentration levels throughout the three zones E1, E2 and E3, charge balance is likely to be maintained predominantly by the presence of Fe^{3+} in addition to Ti^{4+} in octahedral sites. A plot of Σ $(Y + REE)^{3+}$ against Fe^{3+} (fig. 2) shows a linear correlation with a correlation coefficient (r_{corr} = 0.948) which indicates a close interdependency between these cation species, although the charge balance equation will be complicated by the presence of Th^{4+}, Nb^{5+} and W^{6+} (and possibly Ti^{3+}, KESSON et al., 1983) in the structure. The small, highly-charged cations Nb^{5+} (0.064 nm in 6-coordination) and W^{6+} (0.060 nm) will be accommodated in either Ti(I) or Ti(III) sites (Ti^{4+} = 0.0605 nm in 6-coordination).

REE Variation in Zirconolite Zones

There are significant differences in Σ $(REE_2O_3 + Y_2O_3)$ between the three zones with a greater than four-fold increase between zones E1 and E3, E2 being intermediate in composition (Tab. 2). In addition, there is a nearly three-fold increase in the relative proportion of Y_2O_3 between zones E1 and E3 (Tab. 3). Since the ionic radius of Y is similar to those of Dy and Er (Y = 0.1019 nm; Dy = 0.1027 nm; Er = 0.1004 nm, all in 8-coordina-

Tab. 3 Average relative amounts of Y and REE in the three zirconolite zones ($REE_2O_3 + Y_2O_3 = 100\%$)

	E1	E2	E3
Y_2O_3	18.9	36.7	55.2
La_2O_3	5.6	1.3	(<.4)
Ce_2O_3	32.4	11.9	1.8
Pr_2O_3	2.9	2.3	(<.7)
Nd_2O_3	18.3	16.7	3.5
Sm_2O_3	5.6	7.0	4.1
Gd_2O_3	7.1	8.1	6.9
Dy_2O_3	4.6	7.3	12.5
Er_2O_3	4.6	4.7	9.2
Yb_2O_3	(<3)	4.0	6.8

tion), the geochemical behaviour of Y is similar to that of the heavy REE. Thus the fractionation pattern of the REE follows that of Y in the three zones, with the most abundant relative proportions of the REE varying from Ce in zone E1, to Nd in E2 and Dy in E3 (Tab. 3).

Chondrite-normalised (c/n) REE plots for the three zones are presented in fig. 3. Overall, these patterns are broadly similar to published patterns of zirconolites from other localities (e.g. FOWLER and WILLIAMS, 1986), with light

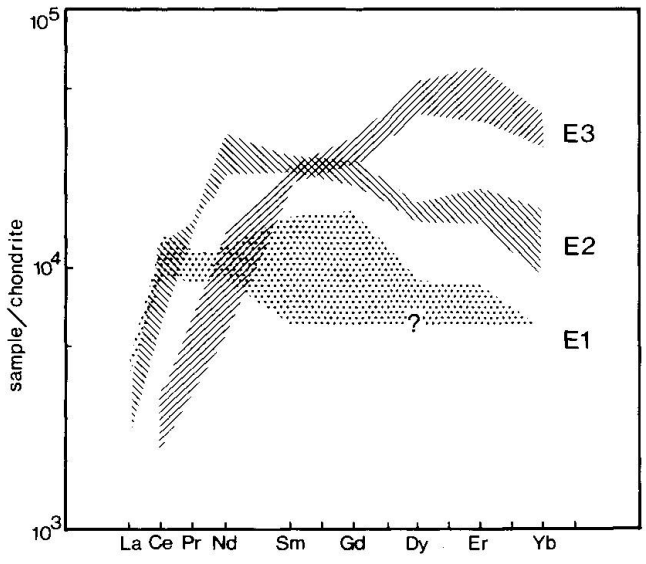

Fig. 3 Chondrite-normalised REE plots for the three zones E1, E2 and E3. The shaded areas represent the range of values within each zone. Chondrite values after WAKITA et al. (1971)

REE depletion and middle or heavy REE enrichment. However, significant differences are observed in the c/n plots for the three zones, and these reflect the chemical variations in REE outlined above. The shaded areas relating to each zone in fig. 3 correspond to the range of values observed within that zone, and the discrete nature and distinctive REE plot of each zone are clearly illustrated by the c/n patterns.

Discussion

Minerals, such as zirconolite, which can accommodate a variety of elements which range both in ionic charge and size, provide useful indicators of chemical changes in metasomatic fluids or magmatic liquids during fractionation or alteration processes. In particular, studies involving the fractionation of the REE have yielded considerable information on a wide range of petrogenetic problems. However, for different fractionation processes, the ratio of light to heavy REE can change in either direction. In magmatic crystallisation, the melt generally becomes enriched in light REE relative to the heavy REE. If crystallisation of zirconolite occurs during this fractionation stage, it can develop continuous zoning, the later growth zones becoming progressively enriched in light REE (e.g. PLATT et al., 1987).

Evidence from metasomatic systems, however, can show a different fractionation trend. In a study of REE mobility from a metasomatically zoned ultrabasic pod from Fiskenaesset, Greenland, FOWLER et al. (1983) showed that heavy REE enrichment occurred at the outer chloritic margins of the pod; and CRESSEY (1987) described the enrichment of heavy REE during crystallisation of three generations of fluor-hydrogarnet in a metachalk marble from Arran, Skye.

In the marble skarn described here, GIERÉ (1986) recognised a step-wise *three-stage* alteration of the spinel to 1) högbomite or corundum + magnetite, 2) margarite, and 3) chlorite. GIERÉ (1986) observed that crystallisation of zirconolite of E1 composition occurred before the chloritisation stage, and suggested that REE and other high valence cations could be transported together with K^+ as complex ions by ligands such as F^- and PO_4^{3-}. The new observations on the zirconolites show the presence of three chemically distinct zones, indicating

that the crystallisation history of zirconolite can be more complex than originally thought. Zone E1, which crystallised before the chloritisation phase (GIERÉ, 1986) also appears from textural evidence to have formed before zones E2 and E3, since these two zones partially, or completely enclose E1 (fig. 1). The crystallisation relationship between E2 and E3 however, is not apparent from textural evidence, since the minerals adjacent to the different zones are always calcite, anorthite or phlogopite. From this evidence, and by analogy with other metasomatic systems described above (FOWLER et al., 1983; CRESSEY, 1987) in which heavy REE enrichment occurs in those minerals crystallising later in the metasomatic sequence, it is suggested that zirconolite zone E3 – with the highest concentration of heavy REE – formed after zone E2, producing a zonal crystallisation sequence of E1 → E2 → E3.

It is suggested therefore, that the development of zones E1 to E3 in the Bergell zirconolite represents a zonal crystallisation sequence, and the distinctive REE composition of the *three* zones reflect changes to the REE composition of the fluid during the *three-stage* alteration of the skarn, there being a progressive enrichment of heavy REE as alteration proceeds.

Conclusion

Three distinct zones were observed in zirconolite grains from the Bergell marble skarn. Each zone has a characteristic chemical, particularly REE, composition. Although a complete crystallisation sequence could not be identified from textural or mineralogical relationships, the changes in c/n patterns and comparisons with other metasomatic systems, indicate a *progressive, but step-wise* evolution of the fluid from light to heavy REE enrichment during formation of the zirconolite.

Thus zirconolite is sensitive to, and reflects changes in the chemistry of the fluid during its evolutionary history – both in metasomatic systems described here, and in magmatic fractionation processes reported in other studies (e.g. PLATT et al., 1987).

Acknowledgements

We are grateful for comments from colleagues at the Department of Mineralogy (British Museum, Natural History), particularly those from Dr. P. Henderson, Dr. G. Cressey and Dr. J. E. Chisholm on an earlier draft of the manuscript. This paper also benefitted from reviews by Drs. Terry Seward (DSIR, New Zealand), Sue Kesson (Australian National University, Canberra), V. Trommsdorff (ETH Zürich), and F. Purtscheller (Universität Innsbruck). One of us (RG) gratefully acknowledges financial support from the Schweizerischer Nationalfonds (No. 2.428-0.87).

References

ÅMLI, R. and GRIFFIN, W. L. (1975): Microprobe analyses of REE minerals using empirical corrections. Am. Mineral. 60, 559–606.

BUCHER-NURMINEN, K. (1977): Hochmetamorphe Dolomitmarmore und zonierte metasomatische Adern im oberen Val Sissone (Provinz Sondrio, Norditalien). Unpubl. Ph. D. thesis, No. 5910, ETH Zürich.

BUCHER-NURMINEN, K. (1981): The formation of metasomatic reaction veins in dolomitic marble roof pendants in the Bergell intrusion (Province Sondrio, Northern Italy). Am. J. Sci. 281, 1197–1222.

CRESSEY, G. (1987): Skarn formation between metachalk and agglomerate in the Central Ring Complex, Isle of Arran, Scotland. Mineral. Mag. 51, 231–246.

FOWLER, M. B. and WILLIAMS, C. T. (1986): Zirconolite from the Glen Dessarry syenite; a comparison with other Scottish zirconolites. Mineral. Mag. 50, 326–328.

FOWLER, M. B., WILLIAMS, C. T. and HENDERSON, P. (1983): Rare earth element distribution in a metasomatic zoned ultramafic pod from Fiskenaesset, West Greenland. Mineral. Mag. 47, 547–553.

GATEHOUSE, B. M., GREY, I. E., HILL, R. J. and ROSSELL, H. J. (1981): Zirconolite, $CaZr_xTi_{3-x}O_7$; structure refinements for near end-member compositions with x = 0.85 and 1.30. Acta Cryst. B37, 306–312.

GIERÉ, R. (1985): Metasedimente der Suretta-Decke am Ost- und Südostrand der Bergeller Intrusion: Lithostratigraphische Korrelation und Metamorphose. Schweiz. Mineral. Petrogr. Mitt. 65, 57–78.

GIERÉ, R. (1986): Zirconolite, allanite and hoegbomite in a marble skarn from the Bergell contact aureole: implications for mobility of Ti, Zr and REE. Contrib. Mineral. Petr. 93, 459–470.

HOGARTH, D. D. (1977): Classification and nomenclature of the pyrochlore group. Amer. Mineral. 62, 403–410.

KESSON, S. E., SINCLAIR, W. J. and RINGWOOD, A. E. (1983): Solid solution limits in SYNROC zirconolite. Nucl. Chem. Waste Manag. 4, 259–265

MAZZI, F. and MUNNO, R. (1983): Calciobetafite (new mineral of the pyrochlore group) and related minerals from Campi Flegrei, Italy: crystal structure of polymignyte and zirkelite: comparison with pyrochlore and zirconolite. Am. Mineral. 68, 262–276.

NICKEL, E. H. and MANDARINO, J. A. (1987, 1988): Procedures involving the IMA Commission on New Minerals and Mineral names, and guide-

lines on mineral nomenclature. Schweiz. mineral. petrogr. Mitt. 67, 185–210. Mineral. Mag. 52, 275–292.

PLATT, R.G., WALL, F., WILLIAMS, C.T. and WOOLLEY, A.R. (1987): Zirconolite, chevkinite and other rare earth minerals from nepheline syenites and peralkaline granites and syenites of the Chilwa Alkaline Province, Malawi. Mineral. Mag. 51, 253–263.

RINGWOOD, A.D. (1985): Disposal of high-level nuclear wastes: a geological perspective. Mineral. Mag. 49, 159–167.

SHANNON, R.D. (1976): Revised effective ionic radii and systematic studies of interatomic distances in halides and chalcogenides. Acta Cryst. A32, 751–767.

WAKITA, H., REY, P. and SCHMITT, R.A. (1971): Abundances of the 14 rare earth elements and 12 other elements in Apollo 12 samples: five igneous and one breccia rocks and four soils. Proc. Second Lun. Sci. Conf., Geochim. Cosmochim. Acta Suppl. 2(2), 1319–1329.

Manuscript received June 27, 1988; manuscript accepted July 27, 1988.